Involvement of aldehyde dehydrogenase 1A2 in the regulation of cancer stem cell properties in neuroblastoma

TRI BUDI HARTOMO[1], THI VAN HUYEN PHAM[2], NOBUYUKI YAMAMOTO[2], SATOSHI HIRASE[2],
DAIICHIRO HASEGAWA[3], YOSHIYUKI KOSAKA[3], MASAFUMI MATSUO[4], AKIRA HAYAKAWA[2],
YASUHIRO TAKESHIMA[2], KAZUMOTO IIJIMA[2], HISAHIDE NISHIO[1,2] and NORIYUKI NISHIMURA[1,2]

Departments of [1]Epidemiology and [2]Pediatrics, Kobe University Graduate School of Medicine,
Kobe 650-0017; [3]Department of Hematology and Oncology, Kobe Children's Hospital, Kobe 654-0081;
[4]Department of Medical Rehabilitation, Kobe Gakuin University, Kobe 651-2180, Japan

Abstract. Despite the introduction of 13-cis-retinoic acid (13-cis-RA) into the current chemotherapy, more than half of high-risk neuroblastoma patients have experienced tumor relapses driven by chemoresistant cancer stem cells (CSCs) that can be isolated by their ability to grow as spheres. Although aldehyde dehydrogenase (ALDH) has been used to characterize CSCs in certain cancers, ALDH remains elusive in neuroblastoma. In the present study, we determined ALDH activity and expression of its 19 isoforms in spheres and parental cells of neuroblastoma. ALDH activity and several ALDH isoforms were consistently induced in spheres of different neuroblastoma cells. While ALDH1A2, ALDH1L1 and ALDH3B2 expression was consistently induced in spheres and associated with the sphere and colony formation, only ALDH1A2 expression was significantly correlated with the poor prognosis of neuroblastoma patients. ALDH1A2 expression was further associated with the growth and undifferentiation of neuroblastoma xenografts and the resistance of neuroblastoma cells to 13-cis-RA. These results suggest that ALDH1A2 is involved in the regulation of CSC properties in neuroblastoma.

Introduction

Neuroblastoma is an aggressive pediatric tumor that accounts for ~15% of all cancer-related deaths in children. It originates from neural crest cells and shows extreme heterogeneity ranging from spontaneous regression to malignant progression. Approximately 50% of neuroblastoma patients are stratified into a high-risk group with the overall survival rate of <40% (1-3). Over the years, two major advances have been incorporated into the current therapy for high-risk patients (4). First, patients treated with the differentiation agent 13-cis-retinoic acid (13-cis-RA) after myeloablative consolidation therapy had a significantly decreased rate of relapse (5). Second, the combination of 13-cis-RA with anti-GD2 antibody and cytokines in maintenance therapy further improved a relapse-free survival rate (6). Despite these improvements, 50-60% of patients who complete these treatments still experience a tumor relapse. As in other cancers, neuroblastoma relapse is primarily driven by chemoresistant cancer stem cells (CSCs) (7-9).

A number of studies have isolated neuroblastoma CSCs as spheres grown in serum-free non-adherent culture used for neural crest stem cell growth (10), side population cells based on the efficient efflux of Hoechst 33342 dye from stem cells used to isolate hematopoietic stem cells (11) and cell-surface marker-positive cells based on the markers associated with stem cell populations in other cancers (12-14). Although these studies provide an important insight into the properties of neuroblastoma CSCs, their definitive markers are still missing.

Aldehyde dehydrogenases (ALDHs) are a family of NAD(P)$^+$-dependent enzymes that catalyze the oxidation of aldehydes to their corresponding carboxylic acids. They not only serve to protect cells from the cytotoxic effects of xenobiotic and intracellular aldehydes such as cyclophosphamide and ethanol, but also generate important carboxylic acids in cellular physiology such as retinoic acid (RA) and γ-aminobutyric acid (GABA) (15). High ALDH activity was first found in hematopoietic stem cells and normal stem cells isolated from a variety of tissues (16) and then detected in CSCs of certain cancers (17,18). Among all 19 ALDH isoforms identified in human cells, several isoforms were proposed as CSC-markers; ALDH1A1 in lung cancer (19), ALDH1B1 in colon cancer (20) and ALDH7A1 in prostate cancer (21). However, ALDH remains elusive in neuroblastoma.

In the present study, we analyzed the ALDH activity and expression of its 19 isoforms in spheres and parental cells of different neuroblastoma cells and found that ALDH1A2 was involved in the regulation of CSC properties in neuroblastoma.

Correspondence to: Dr Noriyuki Nishimura, Departments of Pediatrics and Epidemiology, Kobe University Graduate School of Medicine, 7-5-1 Kusunoki-cho, Chuo-ku, Kobe 650-0017, Japan
E-mail: nnishi@med.kobe-u.ac.jp

Materials and methods

Neuroblastoma cells. BE(2)-C (CRL-2268) cells were obtained from the American Type Culture Collection (Manassas, VA, USA). Human neuroblastoma NBTT1, NBTT2D and NBTT3 cells were previously described (22,23). Tumor tissue samples were obtained from high-risk neuroblastoma patients with written informed consent. The use of human tissues for this study was approved by the Ethics Committee at Kobe University Graduate School of Medicine and conducted in accordance with the Guidelines for the Clinical Research of Kobe University Graduate School of Medicine.

Antibodies. The rabbit anti-PGK1 antibody was purchased from Sigma (St. Louis, MO, USA), rabbit anti-NF-M antibody from Millipore (Billerica, MA, USA), rabbit anti-ALDH1A2 antibody from Atlas antibodies (Stockholm, Sweden) and rabbit anti-NANOG antibody from ReproCELL (Tokyo, Japan).

Expression plasmids. The N-terminal 3xFLAG-tagged expression plasmid with IRES-driven GFP and puromycin markers (pRS-3FLAG-IRES-GFP) was constructed. Briefly, the U6 promoter expression unit of pRS vector (Origene, Rockville, MD, USA) was first replaced with the CMV-promoter expression unit of pCMV6-AC-IRES-GFP vector (Origene) using In-Fusion HD Cloning kit (Takara, Otsu, Japan). The 3xFLAG-tag was then inserted into the SgfI site within multiple cloning sites of the resulting plasmid. The full-length ALDH1A2 cDNA (NM_003888) was amplified by PCR using PrimeStar GXL DNA polymerase (Takara), cloned into pRS-3FLAG-IRES-GFP and sequenced using an ABI PRISM 3100 genetic analyzer (Applied Biosystems, Foster City, CA, USA). Scramble and specific short hairpin RNA (shRNA) expression plasmids (pGFP-V-RS-scramble shRNA, pGFP-V-RS-ALDH1A2 shRNA, pGFP-V-RS-ALDH1L1 shRNA and pGFP-V-RS-ALDH3B2 shRNA) were obtained from Origene and their sequences are listed in Table I.

Real-time RT-PCR. Total RNA from neuroblastoma cells and spheres was isolated with a TRIzol Plus RNA purification kit (Invitrogen, Carlsbad, CA, USA) and reverse transcribed using a QuantiTect Reverse Transcription kit (Qiagen, Valencia, CA, USA) according to the manufacturer's instructions. Real-time RT-PCR was performed as described previously (22). Primer sequences are listed in Table II.

Cell culture and transfection. Parental cells and spheres of BE(2)-C, NBTT1, NBTT2D and NBTT3 cells were cultured as described previously (24). BE(2)-C cells were transfected with expression plasmids using Lipofectamine 2000 transfection reagent (Invitrogen) according to the manufacturer's instructions. Stably transfected GFP-positive cells were selected by 2.0-3.0 μg/ml puromycin (Invivogen, San Diego, CA, USA) and further isolated by using MoFlo XDP (Beckman Coulter, Brea, CA, USA).

ALDH activity. ALDH activity was determined using the Aldefluor kit (Stem Cell Technologies, Durham, NC, USA) according to the manufacturer's instructions. Briefly, neuro-

Table I. shRNA sequences.

Gene name	Accession no.	Sequence (5'-3')
ALDH1A2	NM_003888	#1: ccaataactcagactttggactcgtagca
		#2: tgtgttcttcaatcaaggtcagtgctgca
ALDH1L1	NM_012190	#1: gtggtcaccaaagcaggactcatcctctt
		#2: catccagaccttccgctactttgctggct
ALDH3B2	NM_000695	#1: cagtacctggaccagagctgctttgccgt
		#2: tcatcaaccagaaacagttccagcggctg

ALDH, aldehyde dehydrogenase.

blastoma cells and spheres were dissociated with Accumax (Innovative Cell Technologies, San Diego, CA, USA) and suspended at ~1x10^6 cells/ml in Aldefluor assay buffer containing BODIPY-aminoacetaldehyde (BAAA) in the presence or absence of 15 μM diethylaminobenzaldehyde (DEAB), incubated at 37˚C for 40 min and then treated with 1 μg/ml propidium iodide (PI; Sigma). Flow cytometric analysis was performed using MoFlo XDP. Specific ALDH activity was based on the difference between the presence and absence of DEAB.

Sphere and colony formation. Sphere formation was analyzed as described previously (24). For colony formation, BE(2)-C cells expressing the indicated shRNA or cDNA were mixed in 0.325% SeaPlaque agarose (Lonza, Rockland, ME, USA) in DMEM/Ham's F12 (3:1) (Wako Pure Chemical, Osaka, Japan) with 10% FBS and plated at 1,000 cells/well onto a solidified bottom layer of 0.6% SeaPlaque agarose in DMEM/Ham's F12 with 10% FBS in a 6-well plate. Cells were incubated at 37˚C for 21 days, stained with 0.5 mg/ml 3-(4,5-dimethylthiazol-2-yl)-2,5-diphenyltetrazolium bromide (MTT; Sigma) and photographed. The total number of colonies was counted manually.

Tumor formation. Four-week-old male athymic BALB/cAJcl nu/nu (nude) mice were obtained from CLEA (Shizuoka, Japan). All procedures involving animals were approved by the Animal Care and Use Committee of Kobe University Graduate School of Medicine and carried out in strict accordance with the Guidelines for the Care and Use of Laboratory Animals of Kobe University Graduate School of Medicine. BE(2)-C cells expressing the indicated shRNA or cDNA in 50% Matrigel (BD Biosciences, Franklin Lakes, NJ, USA) were injected subcutaneously into the flank of nude mice at a density of 1x10^5 cells per injection site. Tumor growth was monitored 3 times per week by external caliper and tumor volume (V) was calculated by the formula: $V = 1/2 (L \times W^2)$, where L and W were the greatest longitudinal and transverse diameters (25). Mice were dissected when the greatest diameter of tumor reached 20 mm. Xenograft tumors were fixed in 20% buffered neutral formalin solution (Muto Pure Chemicals, Tokyo, Japan) and embedded in paraffin. Tumor sample was sectioned 4-μm thick, deparaffinized in xylene, rehydrated in alcohol and stained with hematoxylin and eosin (H&E).

Table II. RT-PCR primer sequences.

Gene name	Accession no.	Forward sequence (5'-3')	Reverse sequence (5'-3')
PGK1	NM_000291	ggagaacctccgctttcat	gctggctcggctttaacc
ALDH1A1	NM_000689	tttggtggattcaagatgtctg	cactgtgactgttttgacctctg
ALDH1A2	NM_003888	tgcattcacagggtctactga	tgcctccaagttccagagtt
ALDH1A3	NM_000693	aacccctgcatcgtgtgt	tggttgaagaacactccctga
ALDH1B1	NM_000692	ttctcgagagaaccgtggag	gtccagctcaaaggggttc
ALDH1L1	NM_012190	gaccttccgctactttgctg	ggtctggcctggttgatg
ALDH1L2	NM_001034173	ttgacaaggctgtgcgaat	cccagcagcaatacagttctc
ALDH2	NM_000690	tggatttggacatggtcctc	gatggtttcccgtggtactt
ALDH3A1	NM_001135168	gatccaggagcaggagca	tgtactcgatctcctctaggacgta
ALDH3A2	NM_001031806	agcagagatgaacaccagattc	aggaggttgaacaggatcattc
ALDH3B1	NM_000694	cgcatcatcaaccagaaaca	tctcctgcacatccaccag
ALDH3B2	NM_000695	ttcatcaaccggcaggag	ctccagcatctggttcacaa
ALDH4A1	NM_003748	agagcaaggaccctcagga	cagacagtacaggcccgaag
ALDH5A1	NM_170740	caacgtggaccaggctgta	tgcaccaagaattggtttga
ALDH6A1	NM_005589	gcccctgatggaacattaaa	tccggatgatcgcaaataa
ALDH7A1	NM_001182	gacctatcttgccttctgaaaga	gattccaaccaggcctacg
ALDH8A1	NM_022568	aaccgtcaggtccagcttt	cactatagatgctcttctggacaaa
ALDH9A1	NM_000696	ctccagcattagcctgtggt	agccagtagcaatgcagaaac
ALDH16A1	NM_153329	agacgtccaggccatgtg	gaggcccactcgacaaact
ALDH18A1	NM_002860	tctcgtcctgactgtctaccc	taacaagccattgccacttg

PGK, phosphoglycerate kinase; ALDH, aldehyde dehydrogenase.

Immunohistochemistry. Immunohistochemical staining of neuroblastoma xenografts was performed on the 4-μm thick sections of tumor samples. After antigen retrieval using a conventional steamer with citrate buffer (pH 6.0), the section was immunostained with a primary antibody in REAL antibody diluent (Dako, Glostrup, Denmark). The section was then blocked with peroxidase blocking reagent (Dako) and incubated with EnVision labeled polymer peroxidase (Dako). The immune complex was visualized using 3, 3'-diaminobenzidine (DAB; Dako) as a chromogen and hematoxylin as a counterstain. To quantify the average percentage of immunostained cells, three fields containing ≥300 neuroblastoma cells were randomly selected from each sample. Positive cells were identified microscopically as brown cytoplasmic staining and manually counted.

Other methods. Phase-contrast images were acquired using a BZ-9000E fluorescence microscope (Keyence, Osaka, Japan). Western blotting was performed as described previously (26).

Results

ALDH activity and ALDH isoforms expression are consistently induced in spheres of different neuroblastoma cells. To begin to characterize ALDH in neuroblastoma, NBTT2D, NBTT1 and NBTT3 cells established from distinct high-risk neuroblastoma patients were grown as spheres in a serum-free non-adherent condition as described previously (24).

The ALDH activities in spheres and parental cells were then determined by Aldefluor assay. Higher ALDH activity was constantly detected in spheres compared to parental cells (Fig. 1A and B). Because the ALDH isoform responsible for high ALDH activity measured by Aldefluor assay is specific for each cancer type (18), we next analyzed the fold-change of ALDH isoform expression in spheres compared to parental cells. Among all 19 ALDH isoforms expressed in human cells, ALDH1A2, ALDH1L1 and ALDH3B2 expression was consistently induced in spheres compared to parental cells (Fig. 1C). While the induction of ALDH1A2 expression was not so high in NBTT1 and NBTT3 cells, ALDH1A2 showed the best correlation between mRNA induction and enzymatic activity induction among ALDH1A2, ALDH1L1 and ALDH3B2 isoforms.

ALDH1A2, ALDH1L1 and ALDH3B2 isoforms are associated with the sphere and colony formation in neuroblastoma cells. To gain insight into the function of ALDH isoforms induced in spheres, we first examined ALDH1A2, ALDH1L1 and ALDH3B2 mRNA expression in spheres and parental cells of neuroblastoma BE(2)-C cells. Like NBTT2D, NBTT1 and NBTT3 cells, BE(2)-C cells also showed the induction of expression of these ALDH isoforms in spheres (Fig. 2A). We then generated BE(2)-C cells stably expressing scramble, ALDH1A2, ALDH1L1 and ALDH3B2 shRNA. ALDH1A2 shRNA #2, ALDH1L1 shRNA #2 and ALDH3B2 shRNA #1 achieved effective knockdown and were used in the present
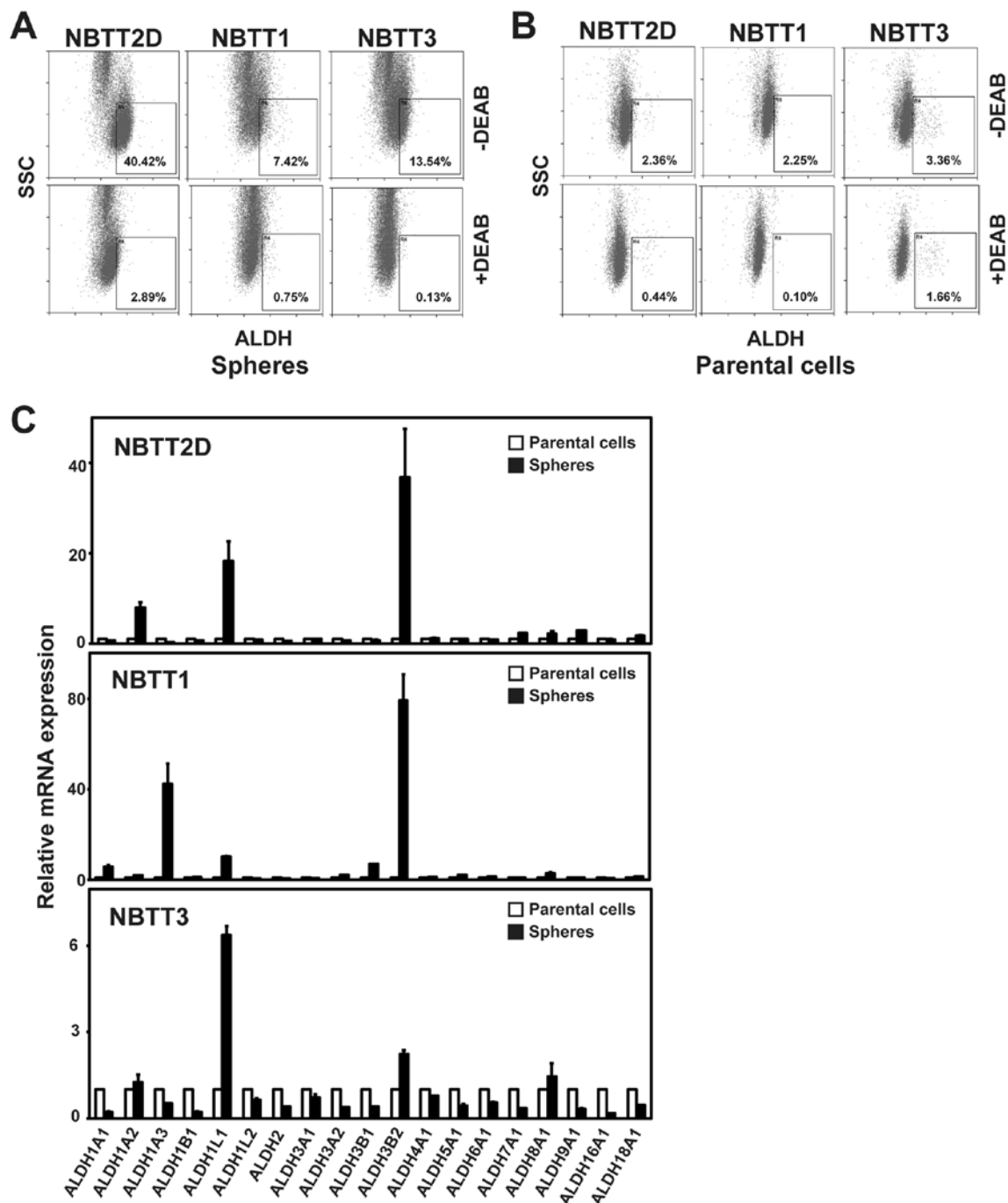
Figure. 1. ALDH activity and ALDH1A2 expression are consistently induced in spheres of different neuroblastoma cells. (A and B) ALDH activities in spheres and parental cells of NBTT2D, NBTT1 and NBTT3 cells were analyzed by flow cytometer using Aldefluor assay. Data were representative of three independent experiments. (C) Relative mRNA expression of 19 ALDH isoforms in parental cells and spheres of NBTT2D, NBTT1 and NBTT3 cells was analyzed by real-time RT-PCR. The mean expression in parental cells was set at 1. Data represented mean ± SD of three independent experiments.

study (Fig. 2B). Next, we performed the sphere and colony formation assays that are widely used to examine the CSC properties *in vitro*. In the sphere formation assay, cells are cultured in a serum-free non-adherent condition so that only cells with ability to self-renew will form spheres. Knockdown of ALDH1A2, ALDH1L1 and ALDH3B2 in BE(2)-C cells significantly impaired the sphere formation (Fig. 2C). In the colony formation assay, cells with a capacity of anchorage-independent growth can grow in soft agar and form colonies. The colony formation was also significantly impaired upon ALDH1A2,

ALDH1L1 and ALDH3B2 knockdown (Fig. 2D). Among these ALDH isoforms, ALDH1A2 knockdown showed the most profound effect on both the sphere and colony formation.

ALDH1A2 expression is correlated with the prognosis of neuroblastoma patients. To further characterize the function of ALDH isoforms induced in spheres, we next analyzed the correlation of ALDH1A2, ALDH1L1 and ALDH3B2 expression with overall survival probabilities of neuroblastoma patients. For this purpose, we used the bioinformatics
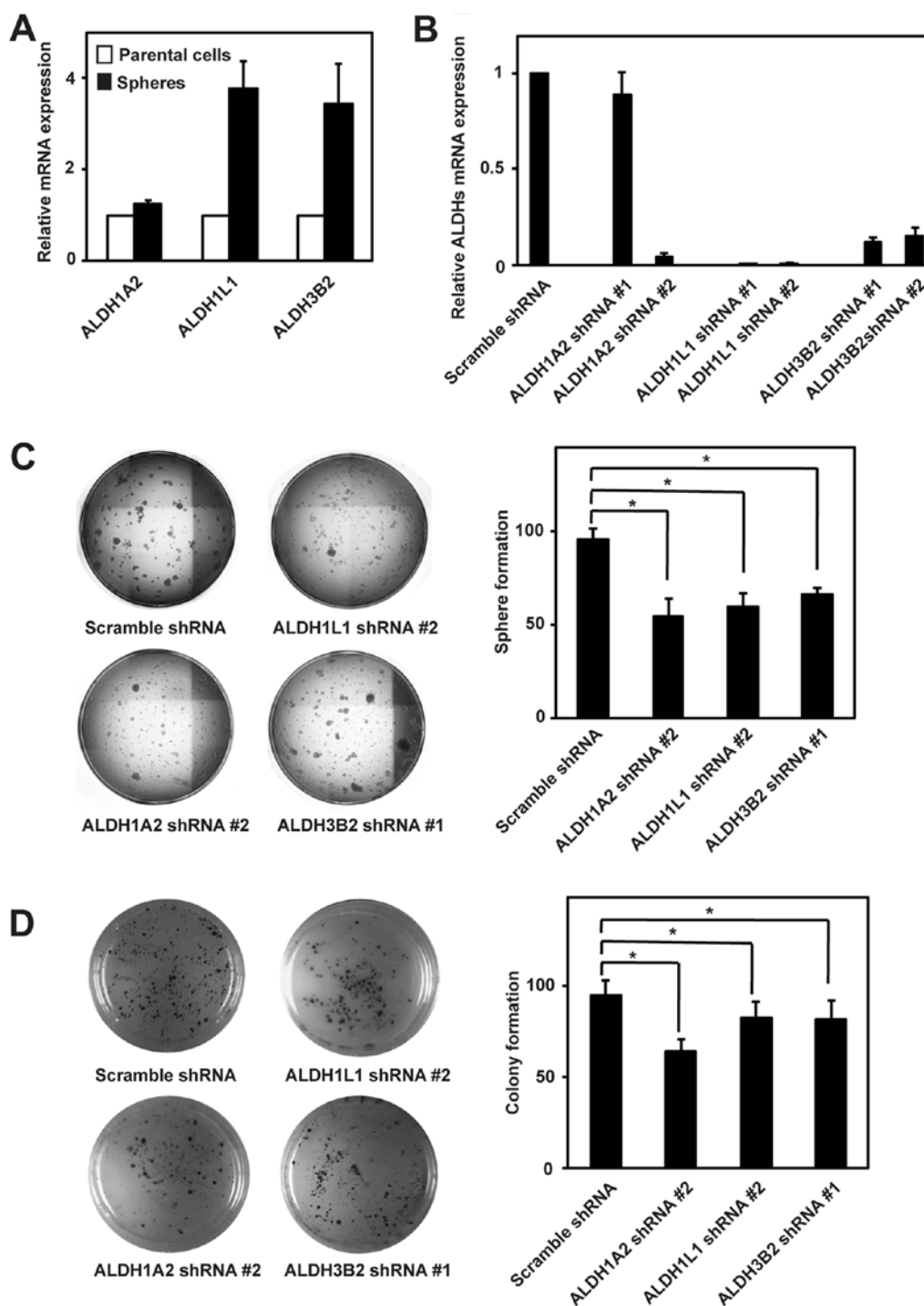
Figure 2. ALDH1A2, ALDH1L1 and ALDH3B2 isoforms are associated with the sphere and colony formation in neuroblastoma cells. (A) Relative mRNA expression of ALDH1A2, ALDH1L1 and ALDH3B2 in parental cells and spheres of BE(2)-C cells was analyzed by real-time RT-PCR. The mean expression in parental BE(2)-C cells was set at 1. (B) Relative mRNA expression of ALDH1A2, ALDH1L1 and ALDH3B2 in BE(2)-C cells expressing scramble shRNA, ALDH1A2 shRNA (#1 and #2), ALDH1L1 shRNA (#1 and #2) and ALDH3B2 shRNA (#1 and #2) was analyzed by real-time RT-PCR. The mean expression in BE(2)-C cells expressing scramble shRNA was set at 1. (C and D) BE(2)-C cells expressing scramble shRNA, ALDH1A2 shRNA #2, ALDH1L1 shRNA #2 and ALDH3B2 shRNA #1 were subjected to the sphere and the colony formation assays. Images are representative of three independent experiments. Data represent mean ± SD of three independent experiments. *P<0.05, Student's t-test.

program R2 (http://r2.amc.nl) and the NB88 dataset (Tumor Neuroblastoma-Versteeg-88-MAS5.0-u133p2) that consisted of 88 primary neuroblastoma tumors of all stages. High expression of both ALDH1A2 and ALDH3B2 was associated with low overall survival probabilities (Fig. 3A and C). In contrast, low ALDH1L1 expression tended to have low overall survival

probabilities (Fig. 3B). Among ALDH1A2, ALDH1L1 and ALDH3B2 isoforms, only ALDH1A2 expression was significantly correlated with overall survival probabilities.

ALDH1A2 is involved in the sphere and colony formation in neuroblastoma cells. Based on the above results, we focused
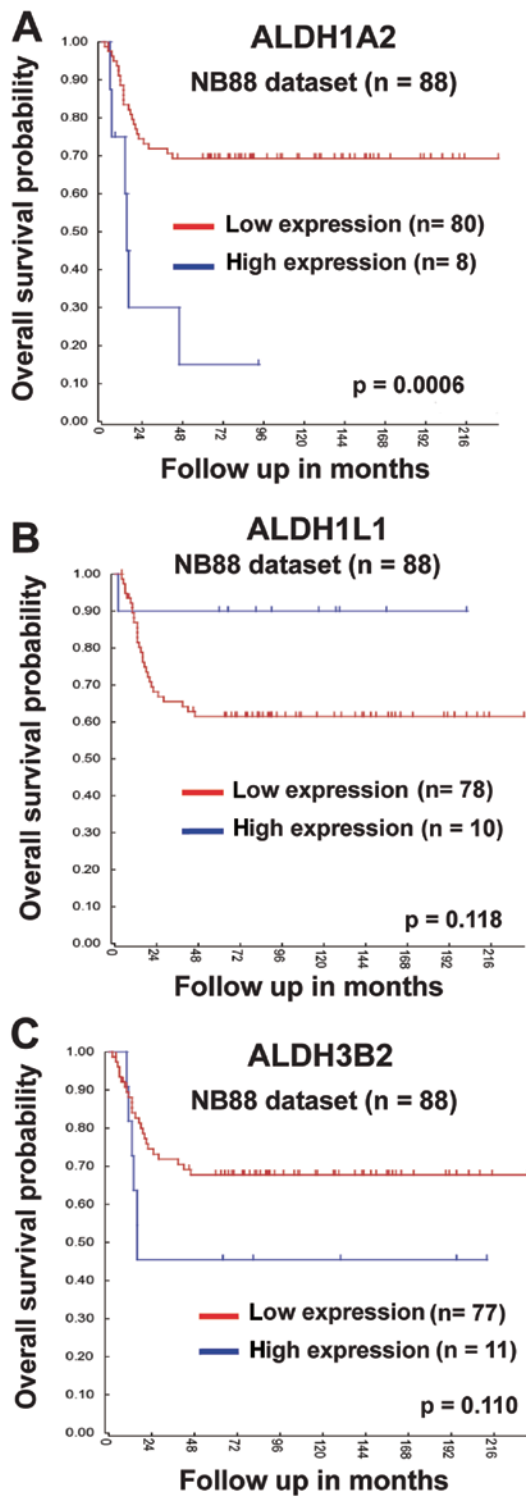
Figure 3. ALDH1A2 expression is correlated with the prognosis of neuroblastoma patients. (A-C) The correlation of ALDH1A2, ALDH1L1 and ALDH3B2 expression with overall survival probabilities was analyzed by the bioinformatics program R2 using the NB88 dataset.
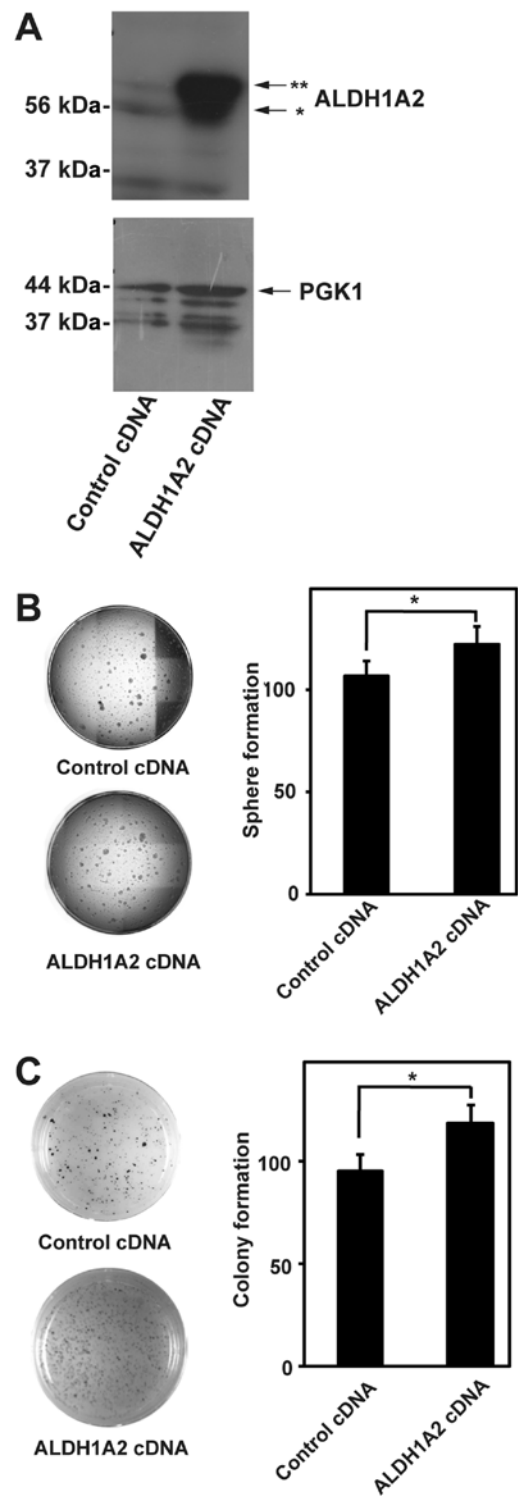

Figure 4. ALDH1A2 is involved in the sphere and colony formation in neuroblastoma cells. (A) Protein expression of ALDH1A2 and PGK1 in BE(2)-C cells stably expressing control cDNA and ALDH1A2 cDNA were analyzed by western blotting using anti-ALDH1A2 and anti-PGK1 antibodies. *Endogenous ALDH1A2 protein. **3xFLAG-tagged ALDH1A2 protein. (B and C) BE(2)-C cells stably expressing control cDNA and ALDH1A2 cDNA were subjected to the sphere and colony formation assays. Images are representative of three independent experiments. Data represent mean ± SD of three independent experiments. *P<0.05, Student's t-test.

on ALDH1A2 isoform in the subsequent study. If ALDH1A2 were involved in the sphere and colony formation in neuroblastoma cells, ALDH1A2 overexpression would promote the sphere and colony formation. To test this possibility, we generated BE(2)-C cells stably expressing ALDH1A2 cDNA. ALDH1A2 overexpression was detected by western blotting (Fig. 4A). The sphere and colony formation were significantly promoted by ALDH1A2 cDNA expression (Fig. 4B and C). These results suggested that ALDH1A2 was involved in the sphere and colony formation in neuroblastoma cells.
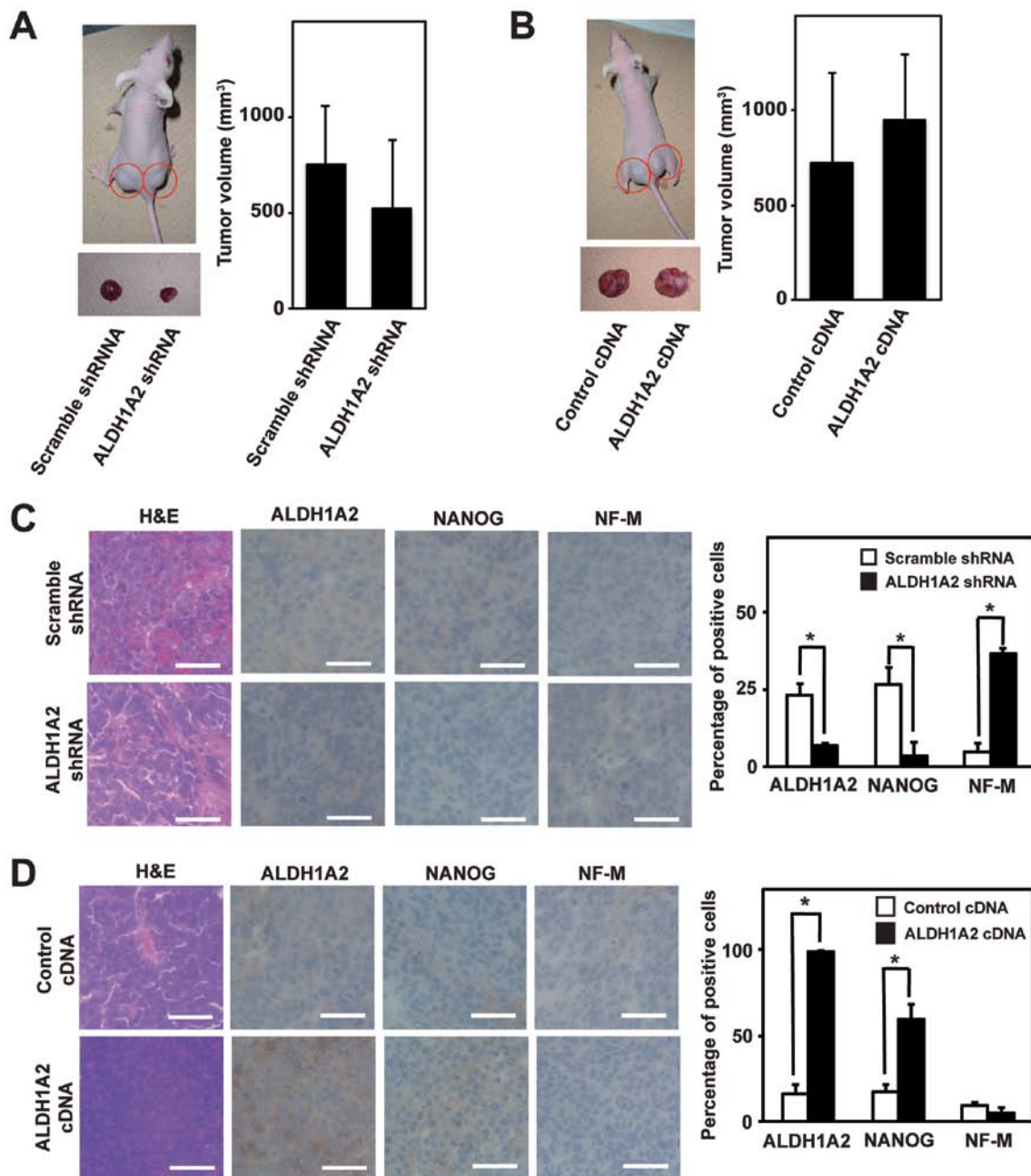
Figure 5. ALDH1A2 is involved in the growth and undifferentiation of neuroblastoma xenografts. BE(2)-C cells stably expressing scramble shRNA, ALDH1A2 shRNA #2, control cDNA and ALDH1A2 cDNA were injected subcutaneously into the flank region of nude mice. (A and B) Tumor volume was measured at 3 weeks after injection. (C and D) Xenograft tumors were subjected to H&E staining and immunostaining with anti-ALDH1A2, anti-NANOG and anti-NF-M antibodies. Scale bars, 50 μm. Immunostained cells were quantitated by manual counting. Images are representative of five mice. Data represent mean ± SD of five mice. *P<0.05, Student's t-test.

ALDH1A2 is involved in the growth and undifferentiation of neuroblastoma xenografts. As CSC is defined as a subpopulation of cancer cells that recapitulates their heterogeneous populations in xenograft tumors, we next examined the function of ALDH1A2 in xenograft tumors. To this end, we injected BE(2)-C cells stably expressing scramble shRNA, ALDH1A2 shRNA, control cDNA and ALDH1A2 cDNA into the flank of nude mice. All mice developed palpable tumors within 10-15 days and tumor volume was determined in 3-4 weeks. Tumor volume tended to decrease upon ALDH1A2 knockdown and to increase upon ALDH1A2 overexpression, albeit it was not statistically significant

(Fig. 5A and B). We then performed the pathological examination with H&E staining. Scramble shRNA and control cDNA tumors showed typical characteristics of a small round cell tumor (Fig. 5C and D). Compared to scramble shRNA tumors, ALDH1A2 shRNA tumors contained more stromal structures and neuronal fibers (Fig. 5C, H&E). In contrast, stromal structures were scarcer in ALDH1A2 cDNA tumors than in control cDNA tumors (Fig. 5D, H&E). The tumors were further examined by immunostaining with antibodies against ALDH1A2, NANOG and NF-M. ALDH1A2-positive cells were reduced in ALDH1A2 shRNA tumors compared to scramble shRNA tumors, whereas they were increased in
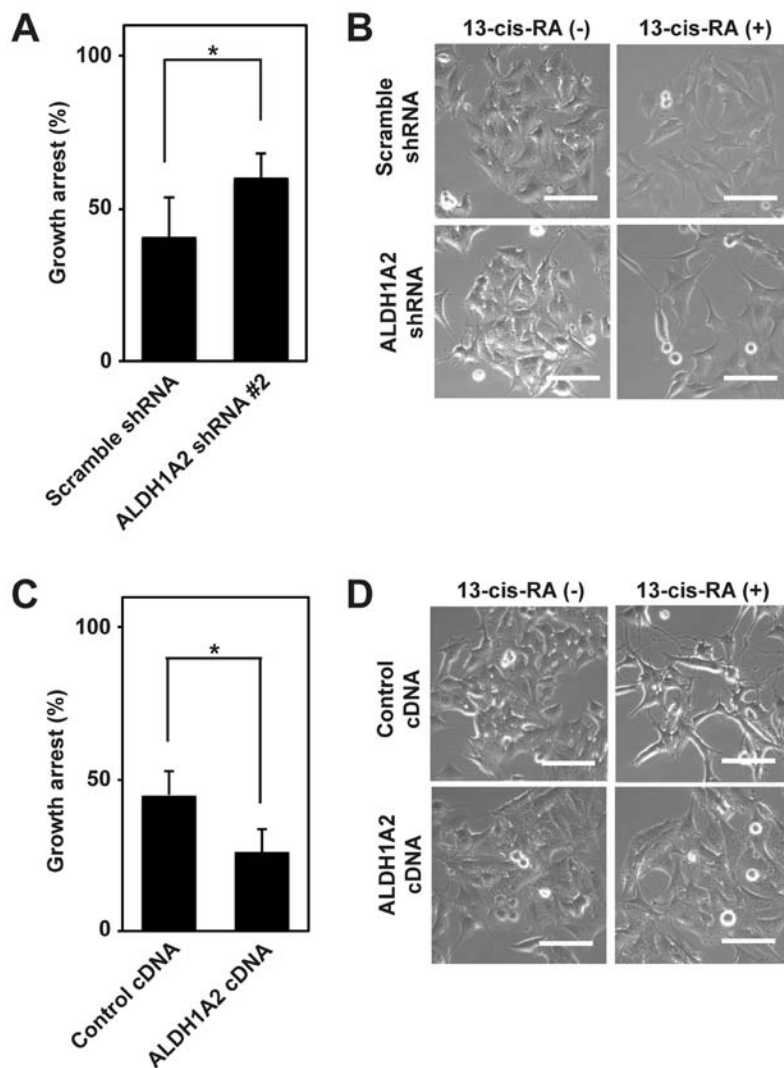
Figure 6. ALDH1A2 is involved in the resistance of neuroblastoma cells to 13-cis-RA. BE(2)-C cells stably expressing scramble shRNA, ALDH1A2 shRNA #2, control cDNA and ALDH1A2 cDNA were cultured in the absence and presence of 13-cis-RA. (A and C) The growth arrest induced by 2.5 μM 13-cis-RA treatment for 72 h was analyzed by counting the cell number in the absence and presence of 13-cis-RA ($N^{Absence\ and\ Presence}$) and expressed as the $N^{Absence-Presence}/N^{Absence}$ x 100 (%). Data represented mean ± SD of three independent experiments. *P<0.05, Student's t-test. (B and D) The differentiation induced by 2.5 μM 13-cis-RA treatment for 48 h (B) or 72 h (D) was analyzed by phase-contrast microscopy. Images are representative of three independent experiments. Scale bars, 50 μm.

ALDH1A2 cDNA tumors compared to control cDNA tumors (Fig. 5C and D, ALDH1A2). ALDH1A2 shRNA tumors showed more differentiated phenotypes with NF-M-positive and NANOG-negative cells than scramble shRNA tumors, while ALDH1A2 cDNA tumors had more undifferentiated phenotypes with NANOG-positive and NF-M-negative cells than control cDNA tumors (Fig. 5C and D, NANOG and NF-M). These data suggested that ALDH1A2 was involved in the growth and undifferentiation of neuroblastoma xenografts.

ALDH1A2 is involved in the resistance of neuroblastoma cells to 13-cis-RA. Because CSC contributed to the chemoresistance in addition to the sphere, colony and tumor formation, we finally examined the function of ALDH1A2 in the resistance of neuroblastoma cells to 13-cis-RA, which is currently used in the maintenance therapy for high-risk neuroblastoma patients. As RA generally induces the growth arrest and differentiation of neuroblastoma cells, we first analyzed the growth arrest induced by 13-cis-RA treatment for 72 h in BE(2)-C cells expressing scramble shRNA, ALDH1A2 shRNA, control

cDNA and ALDH1A2 cDNA. The 13-cis-RA-induced growth arrest was significantly promoted by ALDH1A2 knockdown and inhibited by ALDH1A2 overexpression (Fig. 6A and C). We then investigated their differentiation by phase-contrast microscopy. In scramble shRNA and control cDNA cells, the elongation of neurites started at ~48 h and became evident at ~72 h after 13-cis-RA treatment. Compared to scramble shRNA cells, ALDH1A2 shRNA cells showed more elongated neurites at 48 h after 13-cis-RA treatment (Fig. 6B). In contrast, ALDH1A2 cDNA cells did not elongate the neurites compared to control cDNA cells at 72 h after 13-cis-RA treatment (Fig. 6D). These results suggested that ALDH1A2 was involved in the resistance of neuroblastoma cells to 13-cis-RA.

Discussion

More than half of high-risk neuroblastoma patients experience tumor relapses and no curative salvage therapies for recurrent neuroblastoma are currently known (4). In the present study, we analyzed ALDH activity and expression of its 19 isoforms

in spheres and parental cells of different neuroblastoma cells. Consistent with our present finding that ALDH1A2 was involved in the regulation of CSC properties in neuroblastoma, ALDH1A2 was recently identified as the highest upregulated gene along with marker genes of CD133, ABC transporter, and WNT and NOTCH in neuroblastoma spheres (27).

While ALDH1A2 likely has diverse catalytic and non-catalytic activities in addition to aldehyde metabolizing activity, the physiological role of ALDH1A2 is best exemplified by the association of genetic aberrations with disease phenotypes in both mice and humans. ALDH1A2 knockout mice are embryonic lethal (28), and mutations in ALDH1A2 gene are associated with spina bifida, congenital heart disease and osteoarthritis of the hand (29-31). As ALDH1A2 has the RA-biosynthesis activity by oxidizing retinal aldehyde to RA, these phenotypes might be explained by the aberrant RA-mediated cell signaling that has complex and pleiotropic functions during development (32,33).

Among all 19 ALDH isoforms, other isoforms lacking RA-biosynthesis activities were also upregulated in CSCs of several cancer types (20,21,34). Indeed, ALDH1L1 and ALDH3B2 expression was also consistently induced in CSCs of neuroblastoma. The relation of ALDH1A2 to ALDH1L1 and/or ALDH3B2 in neuroblastoma is currently under investigation.

In addition to ALDH1A2, ALDH1A1, ALDH1A3 and ALDH8A1 can function in RA-signaling by their RA-bio-synthesis activities (18). Although these ALDH isoforms were all expected to augment RA-signaling, their actual roles were likely dependent on the cellular contexts of particular cancer types. For instance, ALDH1A2 was downregulated and proposed as a candidate tumor suppressor in prostate cancer (35,36), whereas ALDH1A3 was upregulated and implicated in the maintenance of CSCs in malignant high-grade gliomas (37).

In neuroblastoma, RA typically induces the differentiation of tumor cells and 13-cis-RA is incorporated into the maintenance therapy for high-risk patients with the purpose of differentiating chemoresistant CSCs (3). However, the response to 13-cis-RA is variable and still unpredictable in the clinic. Our present study adds ALDH1A2 to a growing list of molecules responsible for RA-resistance (38,39) and will provide a possible therapeutic target.

In conclusion, we revealed that ALDH1A2 was involved in the regulation of CSC properties in neuroblastoma. Inhibition of ALDH1A2 deserves further evaluation as a new therapeutic approach against high-risk neuroblastoma.

Acknowledgements

References

1. Brodeur GM: Neuroblastoma: biological insights into a clinical enigma. Nat Rev Cancer 3: 203-216, 2003.

2. Laverdière C, Liu Q, Yasui Y, et al: Long-term outcomes in survivors of neuroblastoma: a report from the Childhood Cancer Survivor Study. J Natl Cancer Inst 101: 1131-1140, 2009.

3. Maris JM: Recent advances in neuroblastoma. N Engl J Med 362: 2202-2211, 2010.

4. Cole KA and Maris JM: New strategies in refractory and recurrent neuroblastoma: translational opportunities to impact patient outcome. Clin Cancer Res 18: 2423-2428, 2012.

5. Matthay KK, Villablanca JG, Seeger RC, et al: Treatment of high-risk neuroblastoma with intensive chemotherapy, radiotherapy, autologous bone marrow transplantation, and 13-cis-retinoic acid. Children's Cancer Group. N Engl J Med 341: 1165-1173, 1999.

6. Yu AL, Gilman AL, Ozkaynak MF, et al: Anti-GD2 antibody with GM-CSF, interleukin-2, and isotretinoin for neuroblastoma. N Engl J Med 363: 1324-1334, 2010.

7. Visvader JE and Lindeman GJ: Cancer stem cells in solid tumours: accumulating evidence and unresolved questions. Nat Rev Cancer 8: 755-768, 2008.

8. Vermeulen L, de Sousa e Melo F, Richel DJ and Medema JP: The developing cancer stem-cell model: clinical challenges and opportunities. Lancet Oncol 13: e83-e89, 2012.

9. Cheung N-KV and Dyer MA: Neuroblastoma: developmental biology, cancer genomics and immunotherapy. Nat Rev Cancer 13: 397-411, 2013.

10. Hansford LM, McKee AE, Zhang L, et al: Neuroblastoma cells isolated from bone marrow metastases contain a naturally enriched tumor-initiating cell. Cancer Res 67: 11234-11243, 2007.

11. Hirschmann-Jax C, Foster AE, Wulf GG, et al: A distinct 'side population' of cells with high drug efflux capacity in human tumor cells. Proc Natl Acad Sci USA 101: 14228-14233, 2004.

12. Takenobu H, Shimozato O, Nakamura T, et al: CD133 suppresses neuroblastoma cell differentiation via signal pathway modification. Oncogene 30: 97-105, 2011.

13. Hsu DM, Agarwal S, Benham A, et al: G-CSF receptor positive neuroblastoma subpopulations are enriched in chemotherapy-resistant or relapsed tumors and are highly tumorigenic. Cancer Res 73: 4134-4146, 2013.

14. Sartelet H, Imbriglio T, Nyalendo C, et al: CD133 expression is associated with poor outcome in neuroblastoma via chemo-resistance mediated by the AKT pathway. Histopathology 60: 1144-1155, 2012.

15. Jackson B, Brocker C, Thompson DC, et al: Update on the aldehyde dehydrogenase gene (ALDH) superfamily. Hum Genomics 5: 283-303, 2011.

16. Kastan MB, Schlaffer E, Russo JE, Colvin OM, Civin CI and Hilton J: Direct demonstration of elevated aldehyde dehydrogenase in human hematopoietic progenitor cells. Blood 75: 1947-1950, 1990.

17. Ma I and Allan AL: The role of human aldehyde dehydrogenase in normal and cancer stem cells. Stem Cell Rev 7: 292-306, 2011.

18. Marcato P, Dean CA, Giacomantonio CA and Lee PWK: Aldehyde dehydrogenase: its role as a cancer stem cell marker comes down to the specific isoform. Cell Cycle 10: 1378-1384, 2011.

19. Sullivan JP, Spinola M, Dodge M, et al: Aldehyde dehydrogenase activity selects for lung adenocarcinoma stem cells dependent on notch signaling. Cancer Res 70: 9937-9948, 2010.

20. Chen Y, Orlicky DJ, Matsumoto A, Singh S, Thompson DC and Vasiliou V: Aldehyde dehydrogenase 1B1 (ALDH1B1) is a potential biomarker for human colon cancer. Biochem Biophys Res Commun 405: 173-179, 2011.

21. van den Hoogen C, van der Horst G, Cheung H, et al: High aldehyde dehydrogenase activity identifies tumor-initiating and metastasis-initiating cells in human prostate cancer. Cancer Res 70: 5163-5173, 2010.

22. Nishimura N, Pham TVH, Hartomo TB, et al: Rab15 expression correlates with retinoic acid-induced differentiation of neuro-blastoma cells. Oncol Rep 26: 145-151, 2011.

23. Pham TVH, Hartomo TB, Lee MJ, et al: Rab15 alternative splicing is altered in spheres of neuroblastoma cells. Oncol Rep 27: 2045-2049, 2012.

24. Nishimura N, Hartomo TB, Pham TVH, et al: Epigallocatechin gallate inhibits sphere formation of neuroblastoma BE(2)-C cells. Environ Health Prev Med 17: 246-251, 2012.

25. Tomayko MM and Reynolds CP: Determination of subcutaneous tumor size in athymic (nude) mice. Cancer Chemother Pharmacol 24: 148-154, 1989.

26. Kanda I, Nishimura N, Nakatsuji H, Yamamura R, Nakanishi H and Sasaki T: Involvement of Rab13 and JRAB/MICAL-L2 in epithelial cell scattering. Oncogene 27: 1687-1695, 2008.

27. Coulon A, Flahaut M, Mühlethaler-Mottet A, *et al*: Functional sphere profiling reveals the complexity of neuroblastoma tumor-initiating cell model. Neoplasia 13: 991-1004, 2011.

28. Niederreither K, Subbarayan V, Dollé P and Chambon P: Embryonic retinoic acid synthesis is essential for early mouse post-implantation development. Nat Genet 21: 444-448, 1999.

29. Deak KL, Dickerson ME, Linney E, *et al*: Analysis of ALDH1A2, CYP26A1, CYP26B1, CRABP1, and CRABP2 in human neural tube defects suggests a possible association with alleles in ALDH1A2. Birth Defects Res A Clin Mol Teratol 73: 868-875, 2005.

30. Pavan M, Ruiz VF, Silva FA, *et al*: ALDH1A2 (RALDH2) genetic variation in human congenital heart disease. BMC Med Genet 10: 113, 2009.

31. Styrkarsdottir U, Thorleifsson G, Helgadottir HT, *et al*: Severe osteoarthritis of the hand associates with common variants within the ALDH1A2 gene and with rare variants at 1p31. Nat Genet 46: 498-502, 2014.

32. Duester G: Retinoic acid synthesis and signaling during early organogenesis. Cell 134: 921-931, 2008.

33. Niederreither K and Dollé P: Retinoic acid in development: towards an integrated view. Nat Rev Genet 9: 541-553, 2008.

34. Patel M, Lu L, Zander DS, Sreerama L, Coco D and Moreb JS: ALDH1A1 and ALDH3A1 expression in lung cancers: correlation with histologic type and potential precursors. Lung Cancer 59: 340-349, 2008.

35. Kim H, Lapointe J, Kaygusuz G, *et al*: The retinoic acid synthesis gene ALDH1a2 is a candidate tumor suppressor in prostate cancer. Cancer Res 65: 8118-8124, 2005.

36. Touma SE, Perner S, Rubin MA, Nanus DM and Gudas LJ: Retinoid metabolism and ALDH1A2 (RALDH2) expression are altered in the transgenic adenocarcinoma mouse prostate model. Biochem Pharmacol 78: 1127-1138, 2009.

37. Mao P, Joshi K, Li J, *et al*: Mesenchymal glioma stem cells are maintained by activated glycolytic metabolism involving aldehyde dehydrogenase 1A3. Proc Natl Acad Sci USA 110: 8644-8649, 2013.

38. Huang S, Laoukili J, Epping MT, *et al*: ZNF423 is critically required for retinoic acid-induced differentiation and is a marker of neuroblastoma outcome. Cancer Cell 15: 328-340, 2009.

39. Hölzel M, Huang S, Koster J, *et al*: NF1 is a tumor suppressor in neuroblastoma that determines retinoic acid response and disease outcome. Cell 142: 218-229, 2010.